MWT Solar Cell Processing by use of isishape® SolarEtch® SiD for Rear Contact and Edge Isolation

Alma Spribille[1], Johannes Greulich[1], Elmar Lohmüller[1], Florian Clement[1], Jan Specht[1], Daniel Biro[1] and Ralf Preu[1], Oliver Doll[2], Christian Tüshaus[2], Werner Stockum[2] and Ingo Köhler[2]
[1]Fraunhofer Institute for Solar Energy Systems (ISE), Heidenhofstrasse 2, 79110 Freiburg i. Brsg., Germany
Phone: +49 (0)761–4588–5535, Fax: +49 (0)761–4588–9250, e-mail: alma.spribille@ise.fraunhofer.de
[2]MERCK KGaA Frankfurter Straße 250, 64293 Darmstadt, Germany
Phone: +49 (0)6151–72–4857, Fax: +49 (0)6151–72–914857, E-mail: ingo.koehler@merckgroup.com

ABSTRACT: MWT (metal wrap through) solar cells allow higher efficiencies, while only requiring two additional process steps. One of these process steps – the contact isolation between the external n-contact on the rear and the rear p-contact is the focus of this work. The possibility of realizing this isolation by the etching paste isishape® SolarEtch® SiD instead of a laser groove, which was presented at this conference two years ago, is investigated further. Moreover, this rear contact isolation is combined with the paste driven edge isolation simultaneously which was relocated to the rear of the solar cell. In addition to the experimental approach, the two isolation technologies as well as an isolation implemented by a thermal oxide, which works as a diffusion barrier and passivates the surface at the same time, were simulated to validate the experimental results.
A proof of concept is given by two MWT cell runs, which show high parallel resistances and indicated higher efficiencies for the isolation by etching paste compared to the isolation by laser grooves. These results are reinforced by the conducted simulation.
Keywords: MWT, Back Contact, Contact Isolation, Edge Isolation

1 INTRODUCTION

MWT (Metal Wrap-Through) solar cells [1, 2] are already addressing the goal of increasing the efficiency while remaining the costs at a low level. MWT solar cells require only two additional process steps in comparison to conventional solar cells: drilling of the vias and contact isolation between the external n-contact and the p-contact on the rear. In most common process sequences for MWT solar cells this rear contact isolation (RCI) is realized by a laser groove, which separates the rear emitter beneath the n-contact and the aluminum back surface field (BSF). A picture of the MWT solar cells processed in this work is presented in **Figure 1**; the cross section of the RCI is shown in Figure 2. The laser RCI is a fast and simple process, but the laser groove is about 30 µm wide and 20 to 30 µm deep and therefore causes damage in the base. Furthermore it only cuts through the emitter and leaves part of the emitter short-circuited to the BSF. In order to overcome these disadvantages, this paper focuses on an alternative for the laser groove technique: an etching groove realized with the etching paste isishape® SolarEtch® SiD [3] developed by MERCK KGaA. One major advantage of the etching groove is its minimal depth of only about 1.5 µm.

In addition to the previous investigations this paper also looks at the combination of rear edge and rear contact isolation both realized with the etching paste, while increasing the aluminum covered area on the rear up to 500 µm to the edge. Additionally to the experimental approach of developing a technical alternative to the laser groove a simulation of different techniques for contact isolation of the MWT solar cells was carried out.

2 EXPERIMENTAL APPROACH

2.1 Combination of edge and contact isolation

The MWT cell structure processed in the presented experiments is shown in **Figure 1**.

Figure 1: Picture of a MWT solar cell with the design favored by Fraunhofer ISE. The upper half shows the front of the cell. The lower half shows the rear with the external n-contact pads below the pseudo-busbar on the front and the p-contact pads with direct contact to the aluminum.

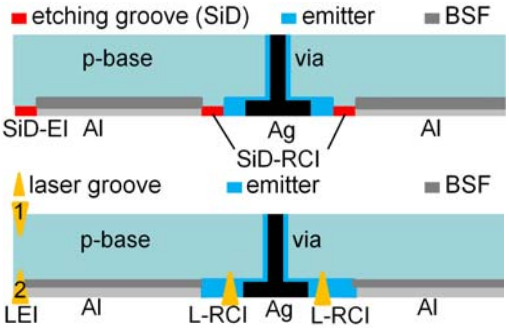

Figure 2: Top: Draft of the cross-section of the edge and contact isolation of the MWT solar cell runs using the etching paste isishape® SolarEtch® SiD. For the SiD-RCI the exposed etching groove is about 300 to 400 µm, the width of the exposed emitter is between 200 and 300 µm. The exposed etching groove on the edge of the wafer (SiD-EI) is approximately 200 to 300 µm wide. Bottom: Draft of the cross-section of the edge and contact isolation using laser for EI and RCI (LEI, L-RCI). The gap between laser groove and Ag as well as cell edge is approx. 200 µm. In the first cell run the LEI was on the front (1), in the second run on the rear (2).

In earlier experiments the dispensable etching paste [4] has shown promising results [3] on the contact isolation of MWT cells. Based on these results the existing process has been improved and combined with edge isolation by the etching paste, which allows the isolation of MWT cells without any laser process. The dispensing process of the etching paste for the edge isolation is to some extent self-aligning due to the surface tension of the paste. This behavior suggests, that an extension of the aluminum BSF might be possible, which would improve the solar cell's open circuit voltage V_{OC} and thereby allowing higher efficiencies. Typically the aluminum on the rear of solar cells has a distance of 1 mm to the edge of the cell. The etching groove is about 600 µm wide, ideally the aluminum is printed with an overlap to the etching groove to minimize the exposed base and thereby reducing j_{01}.

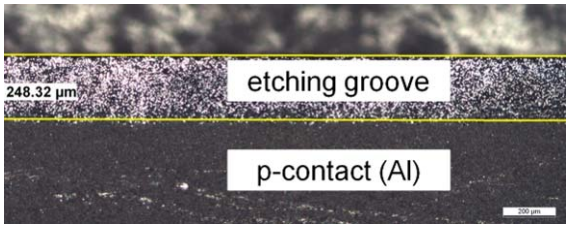

Figure 3: Optical microscopic picture of a wafer edge with an edge isolation by etching paste. The aluminum was printed with a gap of 500 µm to the wafer edge. The relative low viscosity of the aluminum paste allows the paste to approach as far as 250 µm to the wafer edge. This leaves a gap of 250 µm of exposed etching groove only.

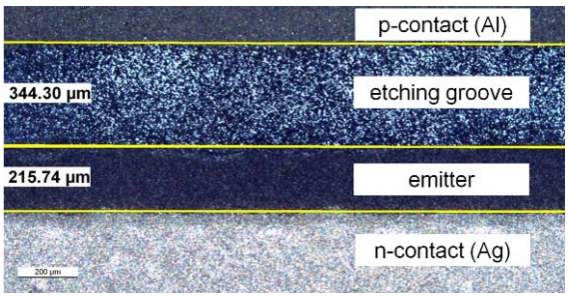

Figure 4: Optical microscope picture of a rear contact isolation with etching paste. The gap between p- and n-contact is supposed to be 600 µm.

While the enlargement of the BSF of up to 250 µm close to the wafer edge is an advantage for the cell, it also most likely forces the laser edge isolation to stay on the front of the solar cell as the gap between the aluminum and the wafer edge might be too narrow to allow a reliable isolation at the rear. If the laser strikes the aluminum it causes a short circuit between emitter and BSF.

2.2 Description of the experiments

The two MWT cell runs presented in this paper were carried out using the cell design shown in Figure 1 and processed on Cz-Si with an edge length of 156 mm, a thickness of 200 µm and a diameter of 205 mm. The base resistivity in the first cell run was between 3 and 6 Ωcm; in the second cell run presorted material with a base resistivity of 2.4 Ωcm was used. All cells were fabricated using industrial equipment and processes in the PV-TEC [5]. All cells featured the same front and rear design with an enlarged BSF. The distance between aluminum and n-contact pad was 600 µm (s. Figure 4). The distance between laser and aluminum as well as between laser and wafer edge was 200 µm. The distance between n-contact pad and etching groove or thermal oxide was approximately 350 µm respectively.

The first cell run 'laser vs. etching paste' consisted of two groups. The group 'L-RCI+LEIS' featured rear contact isolation (RCI) by laser groove and laser edge isolation (LEI) on the front, this group worked as a reference. The second group 'SID+SID' featured rear contact isolation and edge isolation on the rear by the etching paste isishape® SolarEtch® SiD (SiD). The results are presented in the subchapter 4.1.

The second cell run 'variation of isolation techniques' consisted of three groups. Presorted material with a base resistivity of 2.4 Ωcm was used. All three groups got the edge isolation on the rear for a fair comparison; also in each group one isolation technology was used for contact and edge isolation. The first group 'Laser' is the reference, the second group 'SiD' is isolated by etching grooves, the third group 'Oxide' was processed with a structured thermal oxide, which served as a barrier during the emitter diffusion and stayed on the wafer. The results are presented in 4.2. After analyzing the results of the second cell run subsequent LEI and afterwards laser RCI were performed to receive more information about the influence of the cell edge (s. 4.3).

3 SIMULATION

In order to analyze the impact of the three aforementioned rear contact isolation technologies (etching paste, laser and thermal oxide) without the interference to other processes, a two-dimensional simulation of metal wrap through solar cells has been carried out. The general approach has been described earlier [6] and is based on state-of-the-art models [7]. For the simulation, we assumed a 200 µm thick p-type silicon wafer covered by 75 nm thin SiN_x anti-reflection coating. Besides assuming the actual base resistivity of the manufactured cells of the second experiment (2.4 Ωcm), we performed the simulation for 1, 3 and 6 Ωcm. For the minority carrier lifetime we assumed its parameterization according to the boron-oxygen defect by Bothe with enhancement factor $f = 2$ [7, 8]. An industrial emitter with a sheet resistance of 75 Ω/sq. and an 8 µm deep aluminum back surface field including incomplete ionization [9] were assumed. The contributions of the emitter, the metal-semiconductor contact and the metallization finger to the series resistance were not included in the 2D symmetry element. They were taken into account by assuming a lumped series resistance $R_s = 0.6\ \Omega cm^2$. The width of the n-type pads (emitter diffusion and metallization), that of the diffusion barrier, that of the etched back emitter and that of the laser groove were assumed as stated above in the experimental approach. The surface recombination velocity (SRV) at the rear emitter, at the laser groove and at the etched-back p-type base was chosen according to Altermatt's parameterization of data from Cuevas for bare surfaces.

At the surfaces covered by thermal oxide (th. Ox.) we applied the parameterization of "bare SiO_2 without forming gas anneal" [9]. These values were regarded as rough approximations to the true ones and may be very crude approximations to the reality, especially in the case of the laser grooves, where additional crystal damage might reduce the effective lifetime in the surrounding silicon. The SRV at the metallized surfaces was assumed to be 10^7 cm/s.

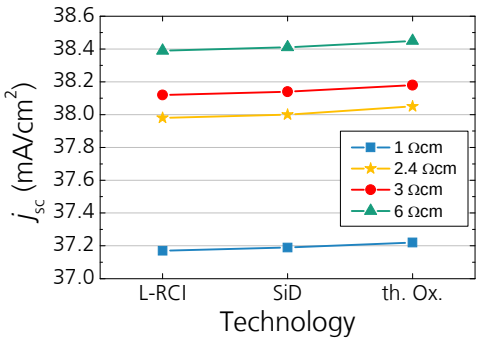

Figure 5: Simulation results for the j_{SC}-effect of the rear contact isolation methods. The x-axis names the rear contact isolation technology; L-RCI is the laser rear contact isolation, SiD is the etching paste and th. Ox. the thermal oxide.

By applying the diffusion barrier the short circuit current density j_{sc} is approximately 0.1 mA/cm² higher compared to both the laser groove and the etching groove. This confirms the findings of the first cell run. The absolute level of j_{sc} decreases with increasing base doping due to a reduced minority carrier lifetime.

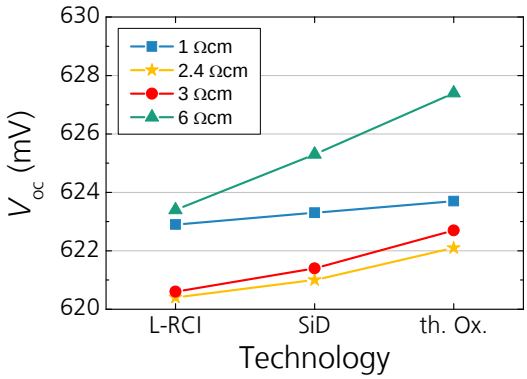

Figure 6: Simulation results for the V_{OC}-effect of the rear contact isolation method.

In terms of open circuit voltage V_{OC} the diffusion barrier yields approximately 1 mV higher values than the etching paste approach, which in turn yields about 0.5 mV higher voltages than the cells with laser rear contact isolation. This again agrees with the findings of the first cell run where both the edge isolation and the rear contact isolation technique were changed and a difference of approximately 1.5 mV was observed (s. 4.1). The simulations showed that the relative differences between the technologies increased as the base resistivity increases. This is caused by the assumed dependence of the SRV on the base doping. The variation of the absolute values of V_{OC} with the base resistance, which is a function of the base doping concentration, may be explained by two opposed effects: (i) Due to the boron-oxygen defect the electron lifetime decreases as the boron doping concentration increases. This shifts the electron quasi-Fermi-level away from the conduction band edge and, therefore, decreases the open circuit voltage. (ii) The hole quasi-Fermi-level shifts towards the valence band edge as the boron doping increases. This increases the open circuit voltage. Between 1 Ωcm and 2.4 Ωcm effect (i) apparently dominates the behavior of V_{OC} whereas between 2.4 Ωcm and 6 Ω cm effect (ii) seems to dominate. The fill factor *FF* exhibited approximately 0.1-1.0%abs. higher values for the diffusion barrier compared to the laser contact isolation. The etching paste approach yielded intermediate values. The decrease of the *FF* with increasing base resistivity is caused by lateral current of majority carriers in the base of the device [5]. The difference between the etching paste and the laser approach of less than 0.5 % is not observed in the experiment, which may be caused by a variation of the series resistance.

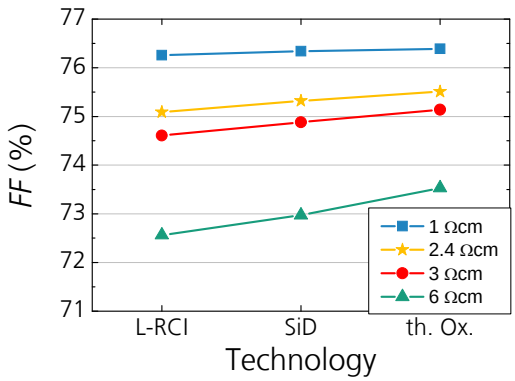

Figure 7: Simulation results for the FF-effect of the rear contact isolation method.

The energy conversion efficiencies demonstrated a similar trend as the fill factors. The diffusion barrier approach results in the highest efficiencies, the laser contact isolation in the lowest. The differences between these two technologies range from less than 0.1% abs. for 1 Ωcm to almost 0.4%abs. for 6 Ωcm. The etching paste approach yields efficiencies in between. The main contributions to these efficiency differences are those of the fill factor and the open circuit voltage.

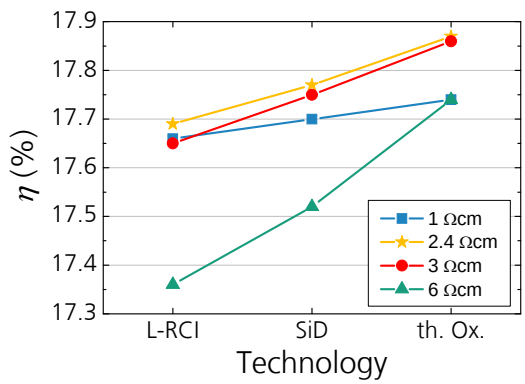

Figure 8: Simulation results for the η-effect of the rear contact isolation method.

4 EXPERIMENTAL RESULTS

4.1 First MWT cell run: Laser vs. etching paste

Figure 9 shows the IV-results of the first cell run (described in 2.2) as processed. In both groups the rear contact isolation (RCI) and the edge isolation (EI) were realized with the same method.

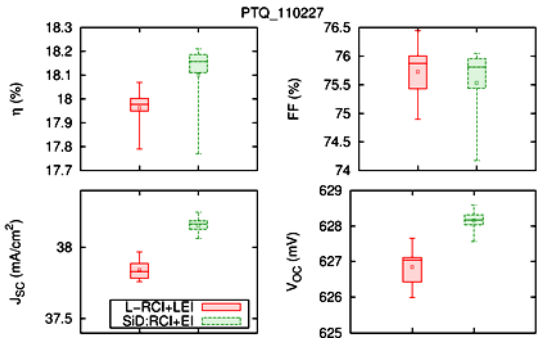

Figure 9: IV-measurement results of the first experiment with contact and edge isolation by etching paste (SiD: RCI+EI) in comparison to laser contact and edge isolation (L-RCI+LEI) as processed. The first abbreviation stands for the method of the contact isolation; L-RCI: laser rear isolation, SiD for isishape® SolarEtch® SiD, the second abbreviation stands for the method of the edge isolation; LEI: laser edge isolation.

The IV-results of the first experiment shown in Figure 9 were very promising. An efficiency of up to 18.2% is a satisfying level for Cz MWT BSF solar cells. The efficiency gain of nearly 0.2% of the etching paste group versus that of merely laser processed one wsd mainly due to the higher open circuit voltage V_{OC} and the higher short circuit current density j_{SC} and thus in good concordance with the results derived from device simulations.

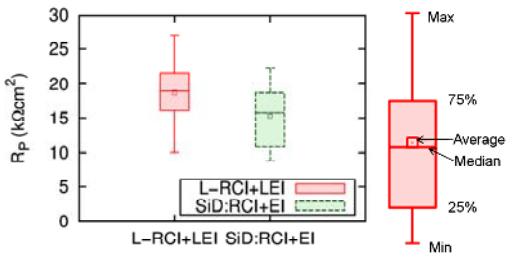

Figure 10: Left: Results for R_P (parallel resistance) of the first experiment with contact and edge isolation by Etching paste in comparison to laser contact and edge isolation. Right: Explanation of the boxplot used.

The j_{SC}-gain of 0.35mA/cm² was partly induced by the replacement of the edge isolation from the front (laser) to the rear (etching paste), which led to an increase of approximately 0.2 mA/cm². This was estimated by calculating the area of the emitter, which was cut off by the laser groove. The distance between the laser groove and the wafer edge was approximately 0.2 mm, this led to a total area loss of about 1.24 cm², which corresponds to 0.52 %. Based on a short circuit current of 38 mA/cm², the current loss created by the laser edge isolation on the front was 0.2 mA/cm². As can be seen in Figure 4 isolation by etching paste lefts no emitter shunted to the BSF. This resulted in higher j_{SC}-values. Anyhow, the simulation results for j_{SC} (*cf.* Figure 5) predicted a slight increase of less than 0.1 mA/cm² only, so that complementary investigations on the discrepancy between simulation and experimental results are mandatory for further insights. Based on the simulation results presented in Figure 6, a base resistivity between 3 and 6 Ωcm resulted in a V_{OC} gain between 1 and 2 mV for etching paste. The gain on open circuit voltage may be explained by less damage to the crystal as well as the wafer surface applying the etching paste. We excluded space charge region recombination as a cause of the V_{OC}-difference since the fill factors *FF* are almost identical for both approaches. The results for the parallel resistance R_P demonstrated sufficiently high values for both isolation methods. Even though the laser isolation showed higher median and peak values, the R_P of all cells was on a very satisfying level above 8 kΩ for MWT solar cells (s. Figure 10).

4.2 Second MWT cell run: variation of isolation techniques

The experiment is described in 2.2. As processed, the cell run exhibited high series resistances, which were caused by the contact between emitter and front side metallization. A short step of light induced plating (LiP) significantly reduced the series resistance. To accomplish comparability the cells were also degraded. The IV-results of this experiment after degradation and LiP are presented in Figure 11.

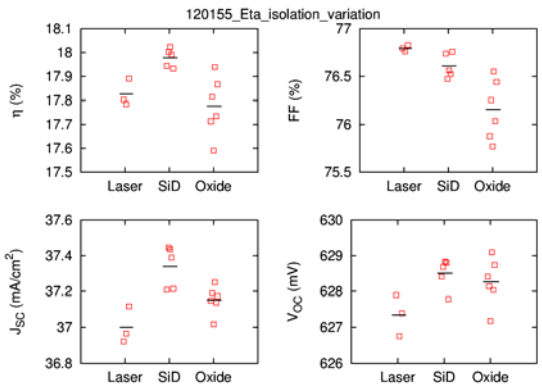

Figure 11: IV-results of the second experiment. The rear contact isolation and the edge isolation are realized with the same technology; 'Laser': laser RCI and LEI; 'SiD': RCI and EI by etching paste; 'Oxide': RCI and EI by thermal oxide as diffusion barrier. All edge isolation processes were carried out on the rear.

With average efficiencies between 17.8 % and 18 % the second experiment presents satisfying efficiencies for degraded MWT solar cells on Cz Si. As can be seen in Figure 11 the highest efficiencies were accomplished with the etching paste. This group showed a gain of approximately 0.15 $\%_{abs.}$, which was significantly more than the predicted 0.07 $\%_{abs.}$ from the outcome of the simulation. However, the simulation regarded the rear contact isolation only; therefore the remaining effect could be caused by the edge isolation itself. The efficiencies of the 'Oxide' group were lower than those

predicted by the simulation; here the main cause was the fill factor. Furthermore, etching paste resulted in the highest j_{SC}- and V_{OC}-values, which was confirmed by the simulation. Only the fill factor revealed a strong discrepancy to the simulation.

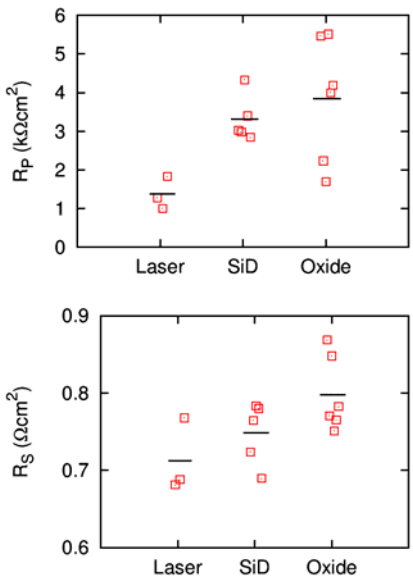

Figure 12: Results of the parallel and the series resistance (R_S and R_P.) of the second MWT cell run.

As can be concluded from Figure 12, elevated series resistance caused the decrease in fill factors of the groups 'SiD' and 'Oxide'. Furthermore, the graph of the parallel resistance demonstrates that the thermal oxide and the etching paste provided more sufficient isolation than the laser grooves. Anyhow, the R_P-values were on a low level. At a first assumption, these low values were attributed to the edges of the cell rather than to the contact isolation method applied. Investigations of the low parallel resistances were carried out and are presented in 4.3,

4.3 Impact of the edge

To find the cause of the low parallel resistances of the second cell run, all three groups received subsequent laser edge isolation and afterwards the groups 'SiD' and 'Oxide' received rear contact isolation by laser. The results of this experiment are presented in Figure 13.

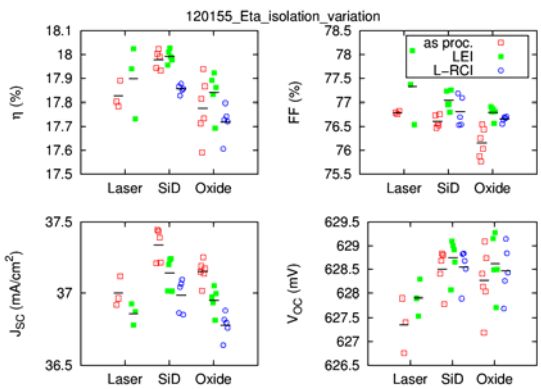

Figure 13: IV-results of the second cell run as processed (as proc.; edge isolation on the rear), after subsequent laser edge isolation (LEI) on the front and after subsequent laser rear contact isolation (L-RCI).

From Figure 13 were concluded that the subsequent laser edge isolation increased the efficiencies of all three groups. The most significant effect was observed on the 'Laser' and the 'Oxide' groups; their efficiencies increased by about 0.08 $\%_{abs.}$. The 'SiD' group presented a slight increase in the efficiency by less than 0.05 $\%_{abs.}$ only. One reason for the increase of the efficiencies were the raised fill factors. The 'Laser' and the 'Oxide' group showed a fill factor increase of approximately 0.6 $\%_{abs.}$, while the 'SiD' group showed an increase of 0.5 $\%_{abs.}$. The V_{OC} of all groups increased only slightly. A more significant change was observed in the j_{SC}. As expected, for all three groups the value of j_{sc} decreased by approximately 0.2 mA/cm^2 which in turn was in agreement with the calculated area loss presented in subchapter 4.2. The additional rear contact isolation by laser for the groups 'SiD' and 'Oxide' had an even more significant impact on their efficiencies post laser treatment. For both groups the efficiencies decreased more than 0.1 %. Both findings were in concordance and thus were attributable to a reduction of the fill factor (0.4 % for 'SiD' and 0.1 % for 'Oxide'), a reduction of the short circuit current density (0.1 mA/cm^2 for 'SiD' and 0.2 mA/cm^2 for 'Oxide') and a very slight reduction of the V_{OC}. These results were in very good concordance with the simulation.

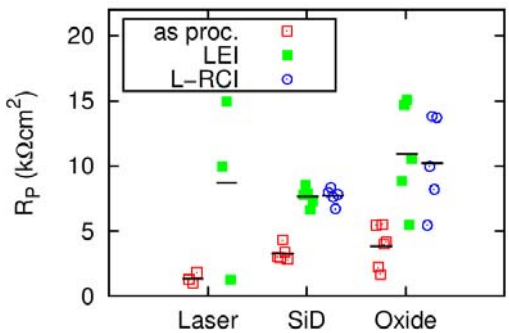

Figure 14: IV-results after subsequent laser edge isolation (LEI) on the front and laser rear contact isolation (L-RCI) for the groups 'SiD' and 'Oxide'.

It was concluded, that the laser edge isolation on the front had a major impact on the parallel resistance. After LEI, the average parallel resistances of all three groups were between 8 kΩcm² and 11 kΩcm². The subsequent L-RCI did not improve the R_P-values any further; this led to the conclusion that the low parallel resistances of the second experiment were caused by the edges of the cell.

5 CONCLUSIONS

The process of rear contact isolation was improved and combined with rear edge isolation by etching paste. Simultaneously the BSF was enlarged by approximately 0.5 mm on each side. A proof of concept of complete isolation by etching paste in combination with an enlarged BSF was given with a first MWT cell run in which the isolation by etching paste resulted in efficiencies of up to 18.2 % and parallel resistances as high as 22.2 kΩ. The results of the first cell run are consistent with the simulation conducted, which showed

a 0.15 % higher efficiency potential for rear contact isolation by etching paste, without regard to the edge isolation. The second MWT cell run showed some problems with the cell's edge. Subsequent laser edge isolation on the front and laser contact isolation on the rear permitted the conclusion that laser edge isolation on the rear in combination with the enlarged BSF did not result in sufficiently high parallel resistances above 5 kΩcm². The etching paste and the thermal oxide provided higher but still not sufficient R_P-values, the subsequent laser edge isolation on the front proved, that the edges of the cell and not the contact isolation technology were the cause. Again contact isolation was successfully realized by etching paste.

5 ACKNOWLEDGEMENTS

Special thanks go to the whole team of the PV-TEC laboratory, for processing and measuring the presented MWT cells. Further thanks go to the whole team of Merck KGaA.

6 REFERENCES

[1] E. van Kerschaver et al., *Proceedings of the 2nd World Conference on Photovoltaic Energy Conversion*, Vienna, Austria (1998), p. 1479-82

[2] F. Clement et al., *Proceedings of the 23th European Photovoltaic Solar Energy Conference*, Valencia, Spain (2008), p. 1871-4

[3] Spribille et al., Proceedings of the 25th *European Photovoltaic Solar Energy Conference*, Valencia, Spain (2010), p. 2654-8

[4] O. Doll et al., *Proceedings of the 24th European Photovoltaic Solar Energy Conference*, Hamburg, Germany (2009), p. 1762-6

[5] D. Biró et al., *Proceedings of the 24th European Photovoltaic Solar Energy Conference,* Hamburg, Germany, (2009), p. 1901-5

[5] T. Fellmeth et al., *Proceedings of the 25th European Photovoltaic Solar Energy Conference*, Valencia, Spain (2010), p. 2201-6

[7] P. P. Altermatt et al., *Journal of Computational Electronics*, (2011), V. 10, p. 314-30

[8] K. Bothe et al., *Progress in Photovoltaics: Research and Applications*, (2005), V. 13, p. 287-96

[9] M. Rüdiger et al., *Journal of Applied Physics*, (2011), V. 110, p. 024508

[10]P. P. Altermatt et al., *Journal of Applied Physics*, (2011), V. 92, p. 3187-97